



ELSEVIER

15 December 2001

Optics Communications 200 (2001) 381–387

---

---

OPTICS  
COMMUNICATIONS

---

---

www.elsevier.com/locate/optcom

# Vortex–edge dislocation interaction in second-order nonlinear media

D.V. Petrov\*

*Department of Fundamental Chemistry, University Federal of Pernambuco, Recife, CEP 50670-901, Brazil*

Received 19 May 2001; received in revised form 29 September 2001; accepted 17 October 2001

---

## Abstract

Experimental and theoretical results on second harmonic generation with fundamental beams containing both a vortex and an edge phase dislocations are reported. The 3D trajectories in the fundamental and second harmonic beams are calculated for different distances between the dislocations in the input beam. It is shown that each phase dislocation in the second harmonic beam appears as a result of the joint actions of all phase dislocations in the fundamental beam. © 2001 Elsevier Science B.V. All rights reserved.

*PACS:* 42.25.Bs; 42.65.Ky; 42.25.Hz

---

The linear and nonlinear propagation of optical beams with topological dislocations of wave phase front has been studied in the last decade very actively (see, for example, [1–6]). Such dislocations are points or lines on the wave front surface where both the real and the imaginary parts of the complex field amplitude vanish. There are two types of phase defects: a screw dislocation or vortex is a spiral phase ramp around the point of phase singularity, and an edge dislocation is the  $\pi$ -shift in the wave phase located along a line in the transverse plane. The Laguerre–Gaussian mode  $L_{1,0}$  is the example of the field with screw phase dislocation. The Hermite–Gaussian mode  $H_{1,0}$  is

the simplest example of the field with phase edge dislocation.

A wide spectrum of new phenomena gives parametric nonlinear mixing of such waves. Because of the parametric interaction, the energy exchange between the interacting waves is accompanied by the nonlinear phase shift exchange. Hence, spatial positions of the phase dislocations in all interacting waves may undergo transformations.

In the second harmonic generation (SHG) with fundamental frequency (FF) waves which include screw phase dislocations by low input power and large beam width, light experiences the frequency doubling together with generation of phase dislocations in the second harmonic (SH) beam [3,7–15]. The topological charge of the dislocation in the SH wave is dictated by the charge of the input light. In particular, in type I SHG the SH

---

\* Tel.: +55-81-3271-8440; fax: +55-81-3271-8440.  
E-mail address: dvp@npd.ufpe.br (D.V. Petrov).

beam has two times the topological charge of the FF.

The SHG with FF waves containing edge phase dislocations has been more sparsely investigated. The SHG from a nonlinear crystal placed inside the cavity of a ring dye laser which was set to generate the higher-order Hermite–Gaussian modes was observed in [16]. The SH beam had two dark lines in its transversal section when the fundamental beam was the  $H_{1,0}$  mode. However, the mode distribution did not correspond to the  $H_{2,0}$  mode pattern. Recently I showed experimentally and theoretically [17] that the SH beam generated by the FF beam with an on-axis edge dislocation does not contain a double number of edge dislocations although the intensity distribution does contain two grey lines. If the edge dislocation is off-set from the host FF beam centre, the SH beam has one edge dislocation. This dislocation exists only if the edge dislocation in the input FF beam is located at a fixed position.

The propagation dynamics of the vortex in both linear and nonlinear media are affected by any source of phase gradient and (or) intensity gradient (see, for example, [18–20]). In particular, in linear media a vortex moves perpendicular to the background intensity gradient and along the background phase gradient. Therefore one may expect that a vortex and an edge dislocation interact when embedded at the same host beam.

This interaction in a nonlinear defocusing medium was demonstrated in [21]. Both dislocations were created in the input beam and the beam intensity was high enough in order to achieve a soliton-type propagation of the vortex soliton and dark stripe soliton. At the output beam the soliton stripe bends and the vortex soliton itself shift slightly. The initial distance between solitons was larger than the soliton size, therefore the long-scale interaction observed was explained by the presence of a vortex-induced phase difference. By increasing the medium nonlinearity the stripe soliton breaks up into vortices.

However, a vortex and an edge dislocation nested at the the same host Gaussian beam interact propagating even in a linear medium [22,23]. The amplitude- and phase-driven mechanisms are responsible for the interaction. As a result the edge

dislocation breaks up into a pair of vortices, and the beam contains three vortex trajectories, i.e. oriented dislocation lines in three-dimensional space [24–26]. In the nonlinear case during propagation of each phase dislocation the diffraction effect is suppressed due to the nonlinear change of refractive index: they propagate as a vortex dark soliton or as a stripe dark soliton. In the linear case the diffraction is strong. Nevertheless all basic effects observed in the nonlinear case (the stripe bending, the generation of a pair of vortices and the shift of the input vortex) appear also in the linear case.

The aim of this paper is to study the generation of phase dislocations in the SH beam by the SHG with an input FF beam containing both (vortex and edge) types of phase dislocations. Even at the negligible depletion regime when the FF beam is unaffected by the parametric interaction the FF beam contains three vortex trajectories. Such an FF beam propagating in a second-order nonlinear crystal generates parametrically a new set of trajectories in the SH beam. One can assume two possible scenarios of this process. Following the first scenario each trajectory in the FF beam generates a double charge trajectory in the SH beam which then splits into a pair of single charge trajectories. Following the second scenario each trajectory in the SH beam is a result of common action of all three trajectories in the FF beam.

First let us consider experimental results. The setup used in experiments is shown in Fig. 1. A

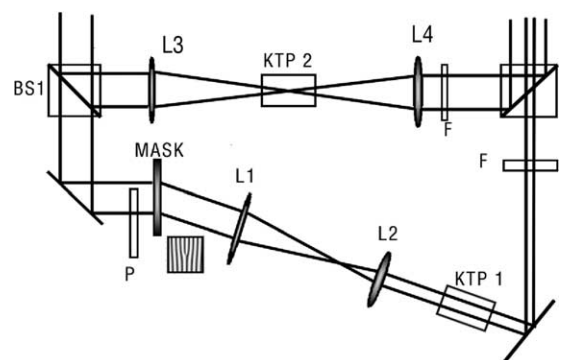


Fig. 1. Experimental set up.

collimated light from a pulsed (10 ns) Nd:YAG laser ( $\lambda = 1.064 \mu\text{m}$ ) was split by a beam splitter BS1. A computer-generated hologram mask MASK [3] produced a vortex in the FF beam. The holographic image of the vortex was initially reconstructed with an 8 mm diameter collimated laser beam. The first-order diffracted beam containing the vortex was spatially filtered with an 80 cm focal length lens  $L_1$  and a pinhole. A second lens  $L_2$  of focal length 10 cm was used to recollimate and reduce the beam to a diameter  $2w_{0\text{exp}} = 0.8 \text{ mm}$  (the Rayleigh length of  $z_0 = \pi w_{0\text{exp}}^2 / \lambda = 48 \text{ cm}$ ) on the entrance of the nonlinear medium (KTP1). Demagnification of the diffracted beam made it possible to increase the input intensity of the FF beam. The nonlinear crystal was placed at the distance  $z_i = 72 \text{ cm}$  from the lens  $L_2$ . The crystal length was  $l = 1.4 \text{ cm}$ . An edge dislocation was created in the input FF beam by a  $\pi$ -jump imposed across the beam by a thin glass plate  $P$  [21,27,28]. Interference of a reference beam with the light passing through the plate was used to adjust the tilt of the plate to ensure a phase shift of  $2\pi n + \pi$  between the two halves of the beam. Both phase dislocations were nested in the input beam by a combined action of two phase masks. The nonlinear crystal was a KTP crystal with a  $5 \times 5 \times 14 \text{ mm}^3$  size. The image of the SH beam at the output plane of the crystal was captured with a CCD camera.

The second FF beam was focused by a lens  $L_3$  with 60 cm focal length inside another KTP crystal (KTP2), and recollimated by a lens  $L_4$ . The SH beam generated by this crystal was used as a reference beam. Filters  $F$  cut the FF beams after the nonlinear crystals. The intensity and phase distribution in the SH beam were studied at different positions  $x_0$  of the edge dislocation relative to the centre of the host Gaussian beam. The vortex was always embedded at the centre of the beam.

Fig. 2 presents the summary of experimental results. At  $x_0 = 0$  one observes a symmetrical intensity distribution of the FF and SH beams. The FF beam contains in this case two single charge vortices and the SH beam includes four single charge vortices of the same sign as in the FF beam (Fig. 2 1a, 2a, 3a, 4a). The fundamental beam

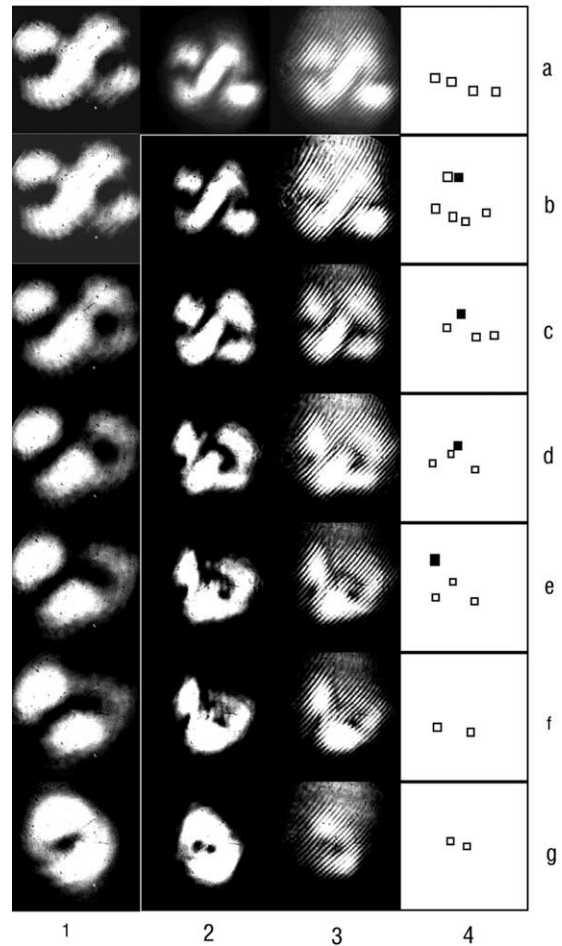


Fig. 2. Experimental results. Intensity distribution in the output FF (1) and SH (2) beams, interferograms of the SH beam (3) and a schematic representation of the location of vortices (positive – open squares, negative – solid squares) in the SH beam (4) at different shifts of the edge dislocation in the input FF beam. Conditions:  $x_0 = 0$  (a),  $x_0 = 0.1w_{0\text{exp}}$  (b),  $x_0 = 0.25w_{0\text{exp}}$  (c),  $x_0 = 0.35w_{0\text{exp}}$  (d),  $x_0 = 0.5w_{0\text{exp}}$  (e),  $x_0 = 0.6w_{0\text{exp}}$  (f), no edge dislocation in the FF beam (g).

suffers distortions of the profile when the edge dislocation moves across the input beam. If the edge dislocation is shifted at  $x_0 = 0.1w_{0\text{exp}}$  there are six vortices in the SH beam (Fig. 2 3b, 4b), four of them with the same sign as in Fig. 2 3a and two vortices of opposite sign. By further increasing of  $x_0$  a complicated dynamics of the vortex pattern is observed that includes movements of the vortices and their annihilation. When there is no edge dislocation in the input FF beam (Fig. 2 1g, 2g, 3g,

4g) a well-studied pattern of two vortices of the same sign is observed [9,11].

The vortex dynamics observed in the experiments may be explained accounting for different processes: a movement of a vortex due to the phase- and intensity-gradient of the background field [18–20], an annihilation of vortices of different signs [18], a walk-off effect [9,11] which is expected to be strong for a *KTP* crystal. The determining effect in our case, of course, has the distortion of the FF beam inside the crystal observed by displacement of the edge dislocation from the beam centre (see Fig. 2 1a–1g). The distortion of the FF profile is due to the interaction of a vortex and an edge dislocation [22,23].

The unambiguous explanation of the experimental results may be done if one knows the vortex trajectories [24–26] both in the FF and SH beams. In order to find vortex trajectories in the SH beam we consider the normalized equations for the evolution process for the slowly varying envelopes of the light waves in type I phase-matching SHG in a bulk quadratic nonlinear crystal with Poynting vector walk-off [29]:

$$i \frac{\partial a_1}{\partial \xi} + \frac{1}{2} \nabla_{\perp}^2 a_1 + a_1^* a_2 \exp(-i\beta\xi) = 0, \quad (1)$$

$$i \frac{\partial a_2}{\partial \xi} + \frac{1}{4} \nabla_{\perp}^2 a_2 - i\delta \frac{\partial a_2}{\partial x} + a_1^2 \exp(i\beta\xi) = 0, \quad (2)$$

where  $a_1$  and  $a_2$  are the normalized amplitudes of the FF and SH beams, respectively. The transverse coordinates are normalized to the FF beam width  $\eta$ , and the scaled propagation coordinate  $\xi$  is normalized to twice the diffraction length of the FF beam  $\xi = z/(2z_0) = z/k_1\eta^2$ . The parameter  $\beta$  is given by  $\beta = k_1\eta^2\Delta k$ , where  $\Delta k = 2k_1 - k_2$  is the wave vector mismatch.  $k_1$  and  $k_2$  are the wave numbers of FF and SH waves, respectively. The parameter  $\delta$  describes the Poynting vector walk-off assumed only for the SH beam and along the  $x$ -direction.

As in the experiments an up-conversion geometry with material and light conditions that yield negligible depletion regime is assumed. Then  $a_1$  is unaffected by the parametric interaction; hence a solution of Eq. (2) can be formally written as [15,30]

$$a_2(x, y, \xi) = i \int_{\xi_i}^{\xi} d\xi' \int_{-\infty}^{\infty} dx' \int_{-\infty}^{\infty} dy' \times a_1(x', y', \xi')^2 e^{i\beta\xi'} \times K(x - x', y - y', \xi - \xi'), \quad (3)$$

where  $K(u, v, w)$  is the walking free-space propagator at the SH frequency, given by

$$K(u, v, w) = -\frac{i}{\pi w} \exp \left[ i \frac{(u + \delta w)^2 + v^2}{w} \right]. \quad (4)$$

$\xi_i$  and  $\xi$  in (4) stand for the propagation coordinates of the input and output planes of the nonlinear medium. To define the FF field inside the nonlinear medium  $a_1(x, y, \xi)$  one should proceed from the experimental geometry of optical scheme. In our geometry the field at the back surface of the collimating lens  $L_2$  is  $a_1(x, y, \xi = 0)$ . This field contains an on-axis vortex and an edge dislocation shifted (in a general way) from the host beam centre. If one represents the field of the edge dislocation as  $(x - x_0)$  [3,17,22,23], the FF beam at  $\xi = 0$  is given by

$$a_1(x, y, \xi = 0) = A_0 \frac{x - x_0}{w_0} \frac{x + iy}{w_0} \exp \left[ -\frac{r^2}{w_0^2} \right]. \quad (5)$$

Here  $w_0$  is the normalized waist of the Gaussian FF beam,  $r^2 = x^2 + y^2$  is the normalized beam radius,  $x_0$  is the normalized shift of the edge dislocation from the host beam centre, and  $A_0$  is the field amplitude. Using the diffraction integral [31] or the substitution method [32] one readily finds that the linear propagation of this field is described by

$$a_1(x, y, \xi) = A_0 \left[ \frac{1}{2} \frac{i\xi_v}{(1 + i\xi_v)^2} + \frac{(x + iy)x}{w_0^2(1 + i\xi_v)^3} - \frac{(x + iy)x_0}{w_0^2(1 + i\xi_v)^2} \right] \times \exp \left[ -\frac{(x^2 + y^2)}{w_0^2(1 + i\xi_v)} \right] \quad (6)$$

with  $\xi_v = 2\xi/w_0^2$ .

The field (6) contains several vortex trajectories. At the range  $0 < \xi < 1.5$  and by  $x_0 = 0$  there are two straight-line trajectories (1) and (2) of the same orientation (indicated by arrowheads) which start from the edge dislocation at  $\xi = 0$

(see Fig. 3(a)). The experimental measurement (see the FF intensity distribution in Fig. 2, 1a and Fig. 3 in [22]) gives a foliation of the field (6) at a given propagation distance and reveals two vortices of the same topological sign.

If  $0 < x_0 < w_0/\sqrt{2}$ , the field contains three trajectories: two of them ((1) and (2)) have the same orientation, and the trajectory (3) has the opposite orientation (Fig. 4(a)). Experimental foliations (Fig. 2 5a and Fig. 3 in [22]) confirm the calculations. At  $\xi^* = x_0/\sqrt{w_0^2/2 - x_0^2}$  the trajectories (2) and (3) collide, however, there are three trajectories out of this propagation coordinate. If  $x_0 > w_0/\sqrt{2}$  the beam contains only one trajectory.

Now let us consider how the FF beam with this set of trajectories generates the SH beam. To find a new set of trajectories in the SH beam we solve numerically (3). Let the nonlinear medium be lo-

cated between  $\xi = \xi_i$  and  $\xi = \xi_f$ , so that the normalized interaction length is  $l = \xi_f - \xi_i$  where both  $\xi_i$  and  $\xi_f$  are positive. Substitution of (6) into (3) and integration over the transverse coordinates yield:

$$a_2(x, y, \xi) = \sum_{j=1}^{10} f_j(x, y, \xi, \xi_i, x_0, w_0), \quad (7)$$

where  $f_j(x, y, \xi, \xi_i, x_0, w_0)$  are the integrals that have a form

$$f_j(x, y, \xi, \xi_i, x_0, w_0) = \frac{1}{(1 + i\xi_v)^{m_j}} \int_{\xi_i}^{\xi} \frac{p_j(x, y, \xi, \delta)}{(1 + i\xi_v')^{n_j}} \exp \left\{ -\frac{2[x + \delta(\xi - \xi') + iy]^2}{w_0^2(1 + i\xi_v')} - i\beta\xi' \right\} d\xi', \quad (8)$$

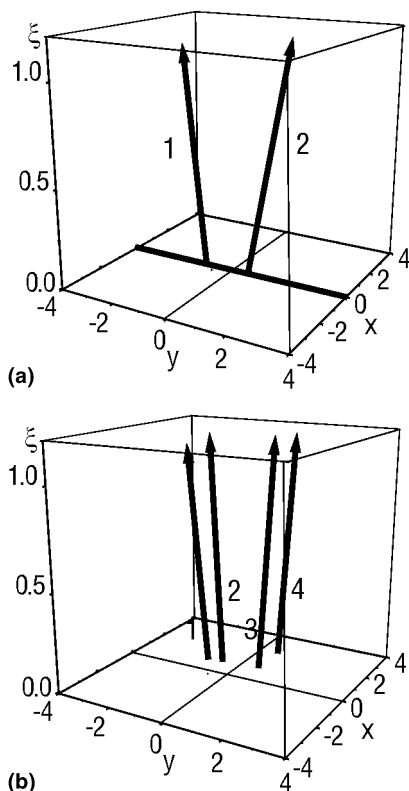


Fig. 3. Calculated trajectories in the FF beam (a) and in the SH beam (b) with  $w_0 = 1$  and  $x_0 = 0$ .

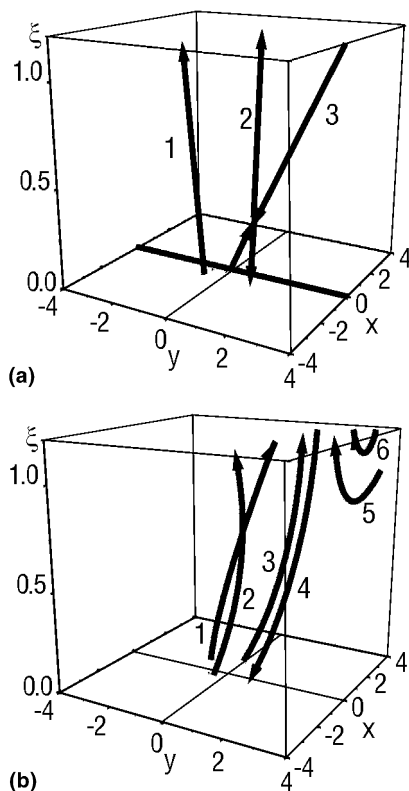


Fig. 4. Calculated trajectories in the FF beam (a) and in the SH beam (b) with  $w_0 = 1$  and  $x_0 = 0.3$ .

Here  $p_j(x, y, \zeta, \delta)$  are the analytical functions, and  $n_j$  and  $m_j$  are the integers ( $n_j \geq 1, m_j \geq 0$ ). If  $\delta = 0$  (no walk-off) the transverse and integration coordinates in  $f_j(x, y, \zeta, \xi_i, x_0, w_0)$  are decoupled, and one obtains an analytical expression for the SH beam. When Poynting vector walk-off is included, the calculations of (7) were done numerically. In the experiments the length of nonlinear medium is small compared to the Rayleigh length, and the walk-off effect weakly affects the beam evaluation. However it is enough to split a double charge vortex into a pair of single charge vortices when no edge dislocation was imposed on the input beam (see Fig. 2 1e–5e).

Numerical simulations of the full governing equations describing the beam propagation (Eqs. (1) and (2)) were performed also with a split-Fourier algorithm [29]. Such numerical simulations gave the same results as predicted by (7) within the resolution that was achievable with split-step meshes. The output results are almost independent of the type of functions used to describe the edge dislocation. It means that the intensity gradient does not contribute considerably in the interaction between the dislocations.

To find the trajectories in the SH beam the precise location of all the dislocations was determined at different propagation distances by numerical harvesting all the complex zeroes of Eq. (7). Notice that for small propagation distances inside the nonlinear medium  $\xi < 0.1$  a topology of the surfaces  $\text{Re}\{a_2\} = 0$  and  $\text{Im}\{a_2\} = 0$  was found to be complicated so that these surfaces do not intersect each other but coincide along surfaces. Figs. 5(a)–(c) show the contour lines  $\text{Re}\{a_2\} = 0$  and  $\text{Im}\{a_2\} = 0$  at the foliation  $\xi = 0.02$ , where a set of limited edge dislocations can be seen (solid lines in Fig. 5(c)). However, when the propagation distance grows the well-defined lines of intersection of these surfaces were found. Figs. 5(d)–(f) show the contour lines  $\text{Re}\{a_2\} = 0$  and  $\text{Im}\{a_2\} = 0$  at the foliation  $\xi = 0.3$ , where four points of zeroes of function  $a_2$  are seen. Such a behaviour of the complex function  $a_2$  does not allow to indicate the origin of the trajectories in the SH beam, and I show the trajectories starting from  $\xi = 0.1$ . Figs. 3(b) and 4(b) illustrate theoretical results for two values of the distance between the edge dislocation and the

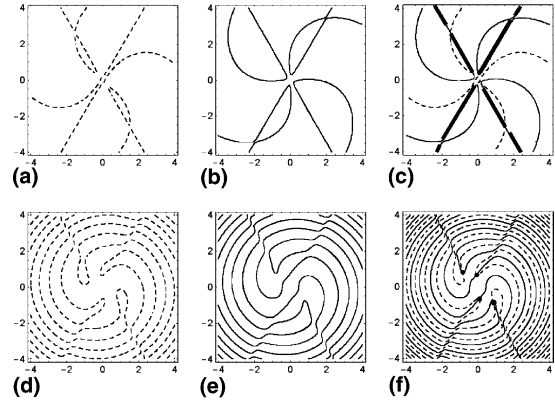


Fig. 5. Calculated equiphase lines  $\text{Im}\{a_2\} = 0$  (dash lines) (a, d) and  $\text{Re}\{a_2\} = 0$  (solid lines) (b, e) in the SH beam at propagation distance  $\xi = 0.02$  (a, b, c) and  $\xi = 0.3$  (d, e, f). (c) and (f) show both the real and imaginary parts at the same plot. Conditions:  $w_0 = 1, \xi_i = 0$ .

vortex in the input FF beam, and permit to compare the sets of trajectories for the FF and SH beams.

If  $x_0 = 0$  the FF beam contains two trajectories of the same orientation (Fig. 3(a)). In the SH beam this set of trajectories generates four trajectories of the same orientation at any propagation distance (Fig. 3(b)). As Fig. 2 2a, 3a, 3b illustrate that, in fact, for the experimental foliation four single charge vortices of the same topological charge are observed. By comparison of the experimental foliations at Fig. 2 with the calculations one should take into account that the crystal length  $l = 1.4$  cm is much smaller than the Rayleigh length of the input FF beam  $z_0 = 48$  cm, and therefore  $\xi \ll 1$ .

If  $x_0 = 0.3$  the FF beam contains three trajectories (Fig. 4(a)). Two of them ((1) and (2)) have the same orientation, and the trajectory (3) has the opposite orientation. The set of trajectories in the SH beam includes four, five or six trajectories depending on the length of nonlinear medium. Four trajectories ((1)–(4)) exist at any crystal length with the orientation of the trajectory (4) being opposite to the orientation of other three trajectories. Two trajectories (5) and (6) have a *U*-like form, and they are responsible for spontaneous generation of pairs of opposite charge vortices observed at foliations made far from the nonlinear medium input. In our case  $\xi \ll 1$ , and the SH beam contains four tra-

jectories with the orientations that give foliations with three vortices of the same sign and one vortex of opposite sign. Such foliations were observed experimentally (see Fig. 2 2c, 3c, 4c and Fig. 2 2d, 3d, 4e).

As seen a change of  $x_0$  produces distortions of the vortex trajectories, changing its orientation and generation of  $U$ -like trajectories. If  $x_0 = 0$  each vortex trajectory in the FF beam gives a pair of trajectories in the SH. However, if  $x_0$  differs from zero each trajectory in the SH beam is a result of a joint action of all trajectories in the FF beam. The parametric process causes the generation of single charge trajectories in the SH beam without intermediate process of double charge trajectory generation.

### Acknowledgements

I am indebted to Prof. W. Strek and Dr. V.K. Sapozhnikov for the supply of *KTP* crystals. A referee's review was very important by writing the revised paper.

### References

- [1] J.F. Nye, M. Berry, Proc. R. Soc. London A 336 (1974) 165.
- [2] N.B. Baranova, B.Ya. Zel'dovich, Sov. Phys. JETP 53 (1981) 925.
- [3] I.V. Basistiy, V.Y. Bazhenov, M.S. Soskin, M.V. Vasnetsov, Opt. Commun. 103 (1993) 422; I.V. Basistiy, M.S. Soskin, M.V. Vasnetsov, Opt. Commun. 119 (1995) 604.
- [4] I. Freund, N. Shvartsman, V. Freilikher, Opt. Commun. 101 (1993) 247; I. Freund, Opt. Commun. 159 (1999) 99.
- [5] N.R. Heckenberg, R. McDuff, C.P. Smith, H. Rubinsztein-Dunlop, M.J. Wegener, Opt. Quantum Electron. 24 (1992) S951.
- [6] G.A. Swartzlander Jr., C.T. Law, Phys. Rev. Lett. 69 (1992) 2503.
- [7] K. Dholakia, N.B. Simpson, M.J. Padgett, L. Allen, Phys. Rev. A 54 (1996) R3742.
- [8] J. Courtial, K. Dholakia, L. Allen, M.J. Padgett, Phys. Rev. A 56 (1997) 4193; J. Arlt, K. Dholakia, L. Allen, M.J. Padgett, Phys. Rev. A 59 (1999) 3950.
- [9] A. Berzanskis, A. Matijosius, A. Piskarskas, V. Smilgevičius, A. Stabinis, Opt. Commun. 140 (1997) 273; A. Berzanskis, A. Matijosius, A. Piskarskas, V. Smilgevičius, A. Stabinis, Opt. Commun. 150 (1998) 372.
- [10] D.V. Petrov, L. Torner, Opt. Quant. Electron. 29 (1997) 1037.
- [11] D.V. Petrov, L. Torner, Phys. Rev. E 58 (1998) 7903.
- [12] P.Di. Trapani, A. Berzanskis, S. Minardi, S. Sapone, W. Chinaglia, Phys. Rev. Lett. 81 (1998) 5133.
- [13] V. Jarutis, A. Matijosius, V. Smilgevičius, A. Stabinis, Opt. Commun. 185 (2000) 159.
- [14] D.V. Petrov, G. Molina-Terriza, L. Torner, Opt. Commun. 162 (1999) 357.
- [15] G. Molina-Terriza, L. Torner, J. Opt. Soc. Am. 17 (2000) 1197.
- [16] T. Hasegawa, T. Shimizu, Opt. Commun. 160 (1999) 103.
- [17] D.V. Petrov, Opt. Commun. 192 (2001) 101.
- [18] G. Indebetouw, J. Mod. Opt. 40 (1993) 73.
- [19] I. Velchev, A. Dreischuh, D. Neshev, S. Dinev, Opt. Commun. 130 (1996) 385.
- [20] D. Rosas, C.T. Law, G.A. Swartzlander, J. Opt. Soc. Am. B 14 (1997) 3054.
- [21] Y.S. Kivshar, A. Nepomnyashchy, V. Tikhonenko, J. Christou, B. Luther-Davies, Opt. Lett. 25 (2000) 123.
- [22] D.V. Petrov, Opt. Commun. 188 (2001) 307.
- [23] D.V. Petrov, Splitting of an edge dislocation by an optical vortex, Opt. Quant. Elec. (2001) (accepted).
- [24] M. Berry, Proc. SPIE 3487 (1998) 1.
- [25] I. Freund, Opt. Commun. 181 (2000) 19.
- [26] I. Freund, D.A. Kessler, Opt. Commun. 187 (2001) 71.
- [27] A.V. Mamaev, M. Saffman, A.A. Zazulya, Phys. Rev. Lett. 76 (1996) 2262.
- [28] V. Tikhonenko, J. Christou, B. Luther-Davies, Yu.S. Kivshar, Opt. Lett. 21 (1996) 1129; B. Luther-Davies, J. Christou, V. Tikhonenko, Yu.S. Kivshar, J. Opt. Soc. Am. 14 (1997) 3045.
- [29] L. Torner, E.M. Wright, J. Opt. Soc. Am. B 13 (1996) 864.
- [30] G. Molina-Terriza, L. Torner, D.V. Petrov, Opt. Lett. 24 (1999) 899.
- [31] R.W. Boyd, Nonlinear Optics, Academic Press, New York, 1992.
- [32] I. Freund, Opt. Commun. 163 (1999) 230.